

ILDNet: A Novel Deep Learning Framework for Interstitial Lung Disease Identification Using Respiratory Sounds

Arka Roy*, Udit Satija
Department of Electrical Engineering,
Indian Institute of Technology Patna, Bihar
E-mail: arka_2121ee34@iitp.ac.in



- What is Interstitial lung disease (ILD)?
- Existing diagnostic modality and challenges
- Respiratory sounds
- Database description
- Proposed framework
- Results
- Conclusion



Interstitial lung disease

- An **chronic** umbrella term used for a large group of diseases that cause **scarring (fibrosis) of the lungs** [1].
- **Airway modification in alveolar interstitium** leads to **impairment in gas exchange** process in blood stream [2].
- **Cause:** Idiopathic pulmonary fibrosis or pneumonia, edema, asbestosis, autoimmune disorder, smoking [2].
- **Symptoms:** Shortness of breath, **crackles**, cough, chest pain.
- **Statistics:** Overall prevalence of ILD rose from **24.7% to 33.6%** between 2005 and 2020 [2] worldwide.

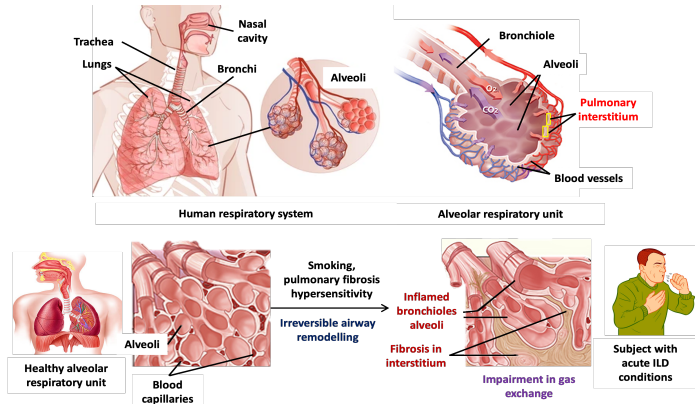
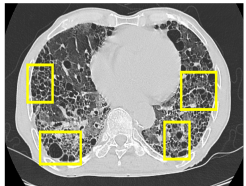
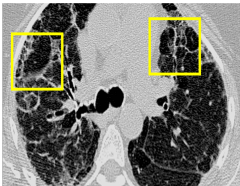


Figure 1: Brief overview of airway remodeling in ILD

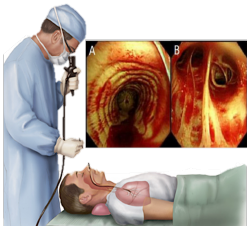
Existing diagnostic modality and challenges



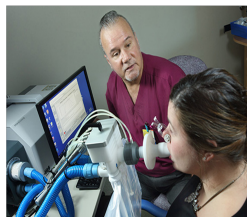
Cystic airspaces or
honeycombing structures



Subpleural reticular thickening, air
trapping and traction bronchiectasis



Nasal bronchoscopic investigation



Pulmonary function test

High resolution CT [3]

Enhanced CT images to assess the lung parenchymal abnormalities such as thickening of interstitium.

Nasal bronchoscopy [4]

An invasive process to analyze the structural changes in the airways such as contraction on bronchus.

Pulmonary function test [5]

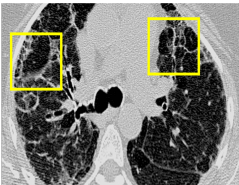
Examines the capacity of lungs,; reduced total lung volume (TLV) suggest ILD.

Figure 2: Different diagnostic modalities to assess ILD conditions

Existing diagnostic modality and challenges



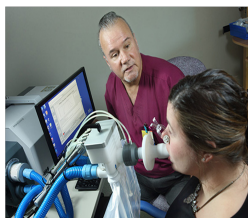
Cystic airspaces or
honeycombing structures



Subpleural reticular thickening, air
trapping and traction bronchiectasis



Nasal bronchoscopic investigation



Pulmonary function test

High resolution CT [3]

Enhanced CT images to assess the lung parenchymal abnormalities such as thickening of interstitium.

Nasal bronchoscopy [4]

An invasive process to analyze the structural changes in the airways such as contraction on bronchus.

Pulmonary function test [5]

Examines the capacity of lungs; reduced total lung volume (TLV) suggest ILD.

Disadvantages

- Exposure to radiation
- Requirement of patient effort and majorly dis-comfortable process
- Very costly diagnostics

Figure 2: Different diagnostic modalities to assess ILD conditions

Respiratory sounds

- Produced by turbulent airflow in trachea-bronchial tree
- Linked to **structural flaws of lungs due to diseases**.
- Typical frequency range 10-2000 Hz [6].

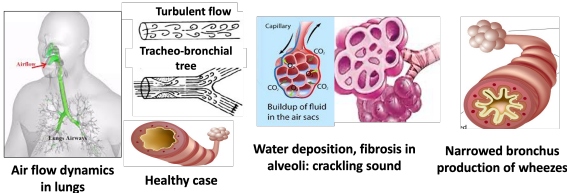


Figure 3: Different air flow dynamics in lungs

Table 1: Description of different lung sounds

Lung sound	Frequency range	Inspiratory/ expiratory	Associated disease
Normal [6], [8]	below 1000Hz	Both	Healthy
Wheeze [6], [7]	200-1800Hz	Expiration or both in severe condition	COPD, asthma
Crackle [8]	100-500Hz	Inspiratory	Pneumonia, fibrosis, edema

Respiratory sounds

- Produced by turbulent airflow in trachea-bronchial tree
- Linked to **structural flaws of lungs due to diseases**.
- Typical frequency range 10-2000 Hz [6].

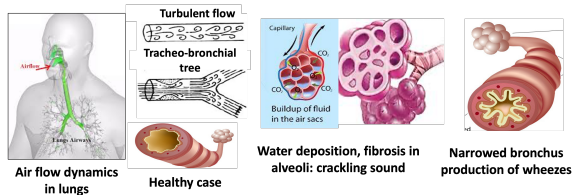
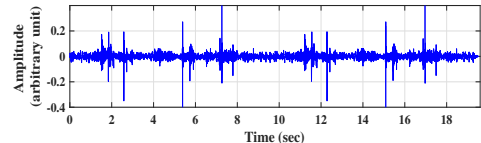


Figure 3: Different air flow dynamics in lungs

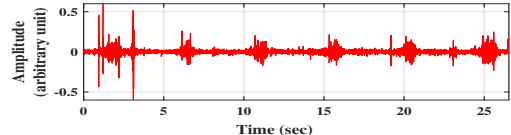
Table 1: Description of different lung sounds

Lung sound	Frequency range	Inspiratory/ expiratory	Associated disease
Normal [6], [8]	below 1000Hz	Both	Healthy
Wheeze [6], [7]	200-1800Hz	Expiration or both in severe condition	COPD, asthma
Crackle [8]	100-500Hz	Inspiratory	Pneumonia, fibrosis, edema

Healthy¹: 



ILD¹: 



¹<https://pro.boehringer-ingelheim.com/auscultation-gallery>

Database description

Table 2: Description of two databases utilized in this ILD detection framework

Particulars	BRACET dataset [9]	KAUH dataset [10]
Acquisition device	Littmann 3200	Littmann 3200
Length of recording	Varies from 15-20 sec	varies from 10-50 sec
Sampling rate	4000 Hz	4000 Hz
Number of recordings in each class	Healthy: 176, COPD: 315, asthma: 94, ILD: 384	Asthma: 96, bronchiectasis: 9, pneumonia: 14, COPD: 38, effusion: 6, healthy: 115
Age (Years)	65.2 ± 13.0	58.6 ± 7.1

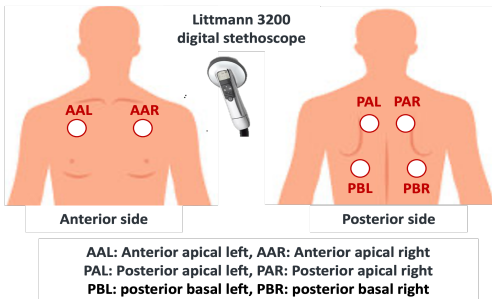


Figure 4: Respiratory sound acquisition sites from anterior and posterior side [9], [10].

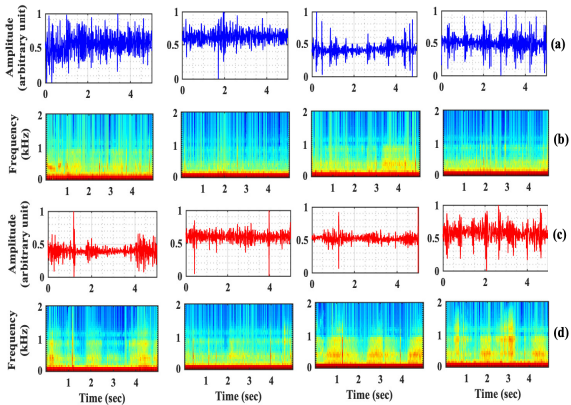


Figure 5: Illustrated the time domain and spectrogram visualization of healthy signals in panel(a,b), and for ILD affected signals in panel (c,d), respectively.

Proposed framework

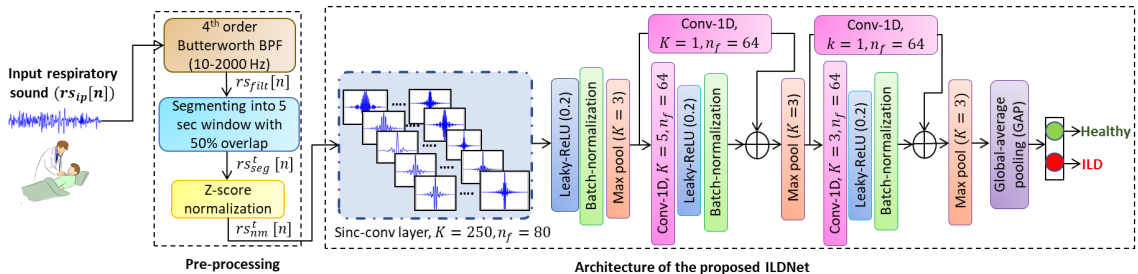
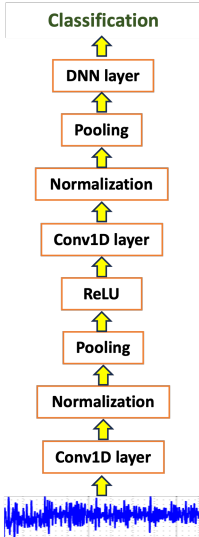


Figure 6: Illustrates the block diagram of the proposed ILDNet framework for ILD classification using respiratory sounds

Proposed framework (Contd.)

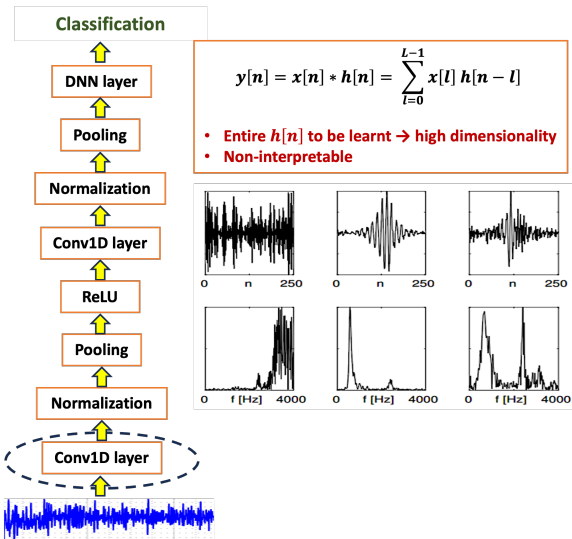
Why Sinc-convolution layer [11] ??



M. Ravanelli et al., "Speaker recognition from raw waveform with SincNet," in *2018 IEEE Spoken Language Technology Workshop (SLT)*, 2018, pp. 1021–1028.

Proposed framework (Contd.)

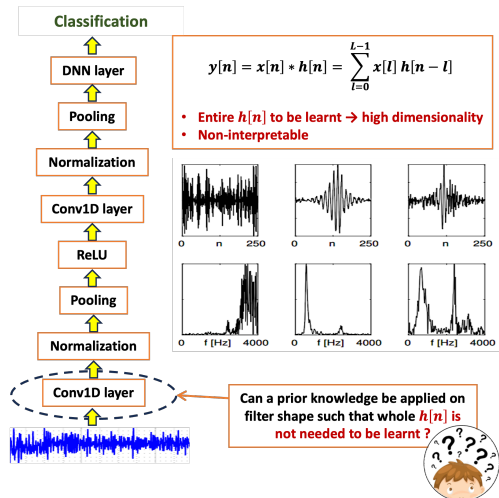
Why Sinc-convolution layer [11] ??



M. Ravanello et al., "Speaker recognition from raw waveform with SincNet," in *2018 IEEE Spoken Language Technology Workshop (SLT)*, 2018, pp. 1021–1028.

Proposed framework (Contd.)

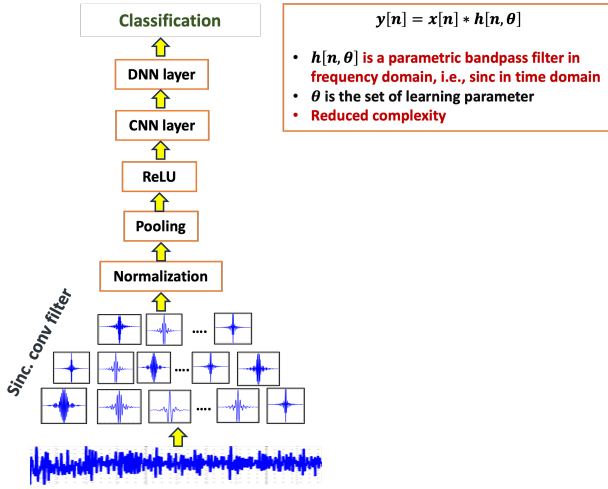
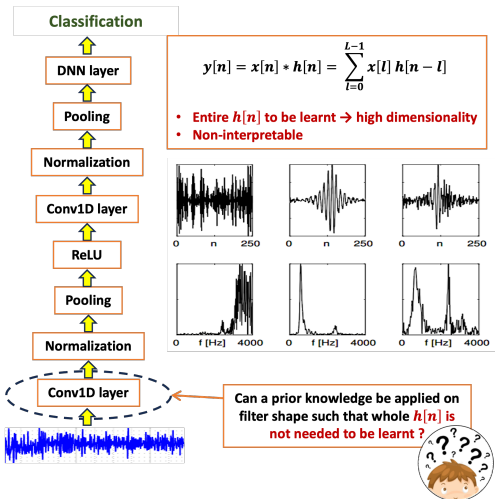
Why Sinc-convolution layer [11] ??



M. Ravanelli et al., "Speaker recognition from raw waveform with SincNet," in *2018 IEEE Spoken Language Technology Workshop (SLT)*, 2018, pp. 1021–1028.

Proposed framework (Contd.)

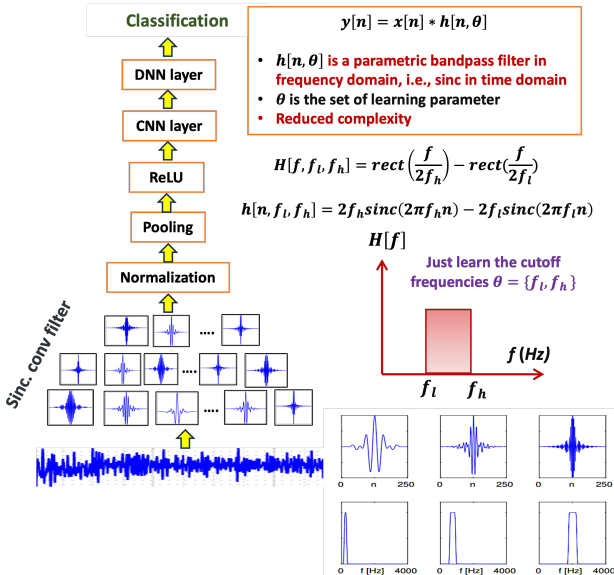
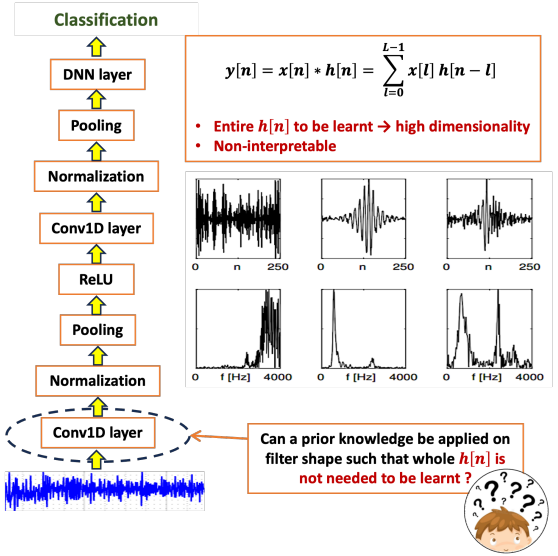
Why Sinc-convolution layer [11] ??



M. Ravanelli et al., "Speaker recognition from raw waveform with SincNet," in 2018 IEEE Spoken Language Technology Workshop (SLT), 2018, pp. 1021–1028.

Proposed framework (Contd.)

Why Sinc-convolution layer [11] ??



Proposed framework (contd.)

ILDNet architecture

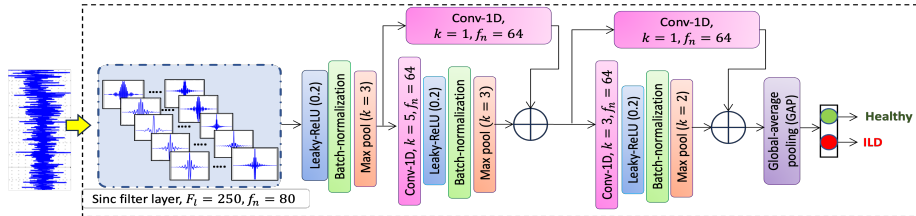


Figure 7: Overall architecture of ILDNet

Table 3: Model Simulation Parameters for ILDNet

Simulation parameter	Details
Learning rate	0.005
Optimizer	Adam
Batch size	64
Trainable parameters	48194
Loss function	Binary cross entropy

Proposed framework (contd.)

ILDNet architecture

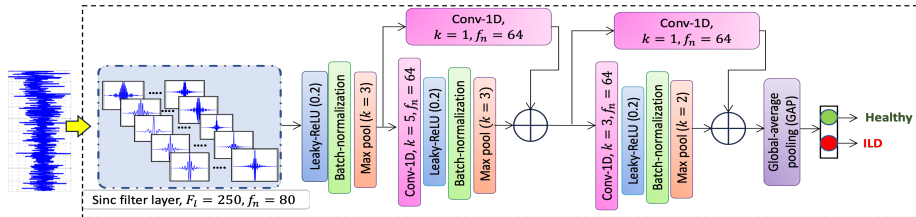


Figure 7: Overall architecture of ILDNet

Table 3: Model Simulation Parameters for ILDNet

Simulation parameter	Details
Learning rate	0.005
Optimizer	Adam
Batch size	64
Trainable parameters	48194
Loss function	Binary cross entropy

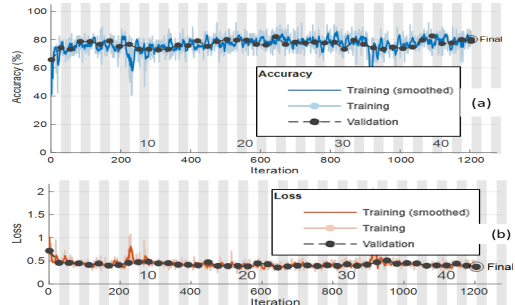


Figure 8: Illustrates the accuracy and loss curves of ILDNet model

Performance metrics: Accuracy (ACC), specificity (SPF), sensitivity (SNS) or recall (RCL), precision (PRE), F1-score, and ICBHI-score.

$$ACC = \frac{T_P + T_N}{T_P + T_N + F_N + F_P}, \quad SNS / RCL = \frac{T_P}{T_P + F_N}, \quad SPF = \frac{T_N}{T_N + F_P}, \quad PRE = \frac{T_P}{T_P + F_P},$$
$$F1 - score = \frac{2 \times PRE \times RCL}{PRE + RCL}, \quad ICBHI - score = \frac{SNS + SPF}{2}$$

Results

Performance metrics: Accuracy (ACC), specificity (SPF), sensitivity (SNS) or recall (RCL), precision (PRE), F1-score, and ICBHI-score.

$$ACC = \frac{T_P + T_N}{T_P + T_N + F_N + F_P}, \quad SNS / RCL = \frac{T_P}{T_P + F_N}, \quad SPF = \frac{T_N}{T_N + F_P}, \quad PRE = \frac{T_P}{T_P + F_P},$$
$$F1 - score = \frac{2 \times PRE \times RCL}{PRE + RCL}, \quad ICBHI - score = \frac{SNS + SPF}{2}$$

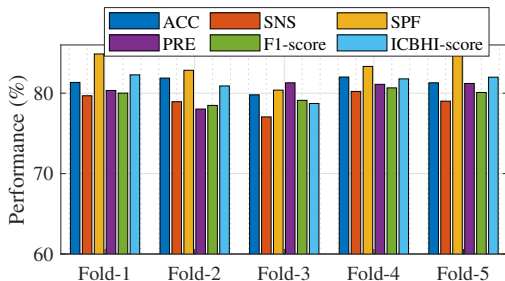


Figure 9: Fold-wise classification performance of ILDNet

Table 4: Average performance after 5-fold CVD

ACC	SNS	SPE	PRC	F1-score	ICBHI score
81.25%	78.55%	83.33%	80.39%	79.61%	81.09%

Results

Performance metrics: Accuracy (ACC), specificity (SPF), sensitivity (SNS) or recall (RCL), precision (PRE), F1-score, and ICBHI-score.

$$ACC = \frac{T_P + T_N}{T_P + T_N + F_N + F_P}, \quad SNS / RCL = \frac{T_P}{T_P + F_N}, \quad SPF = \frac{T_N}{T_N + F_P}, \quad PRE = \frac{T_P}{T_P + F_P},$$
$$F1 - score = \frac{2 \times PRE \times RCL}{PRE + RCL}, \quad ICBHI - score = \frac{SNS + SPF}{2}$$

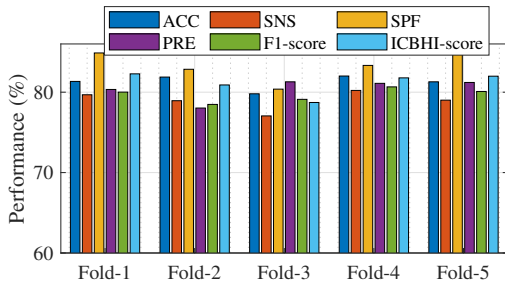


Figure 9: Fold-wise classification performance of ILDNet

Table 4: Average performance after 5-fold CVD

ACC	SNS	SPE	PRC	F1-score	ICBHI score
81.25%	78.55%	83.33%	80.39%	79.61%	81.09%

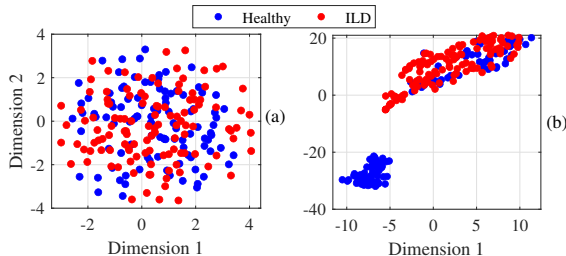


Figure 10: Illustrates the 2D t-SNE visualization of the (a) raw RSs from the test data and (b) the 1D embedding vectors for the same RSs, generated from the GAP layer of ILDNet

Results (Contd.)

Performance comparison wrt baseline CNN (BS-CNN) models

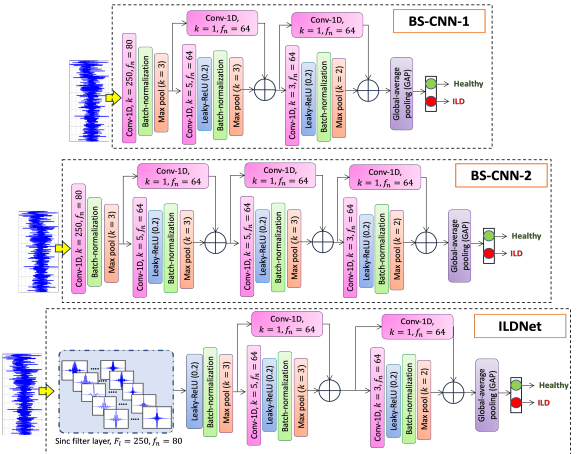


Figure 11: Illustrates the model architecture of BS-CNN-1, 2, and ILDNet

Table 5: Performance comparison of ILDNet wrt baseline CNNs

Model name	Trainable parameters	No of residual block	ACC (%)	SNS (%)	SPF(%)	ICBHI-score (%)
BS-CNN-1	66,891	2	70.53	61.53	78.33	69.93
BS_CNN-2	1,12,279	3	78.51	54.84	87.91	71.37
ILDNet	48,194	2	81.25	78.55	83.33	80.94

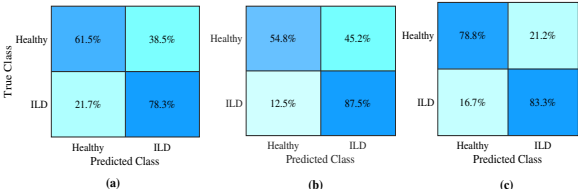


Figure 12: Illustrates the confusion matrix for (a) BS-CNN-1, (b) BS-CNN-2, and (c) proposed ILDNet

Results (contd.)

Class-specific heat-map visualization and overall performance comparison

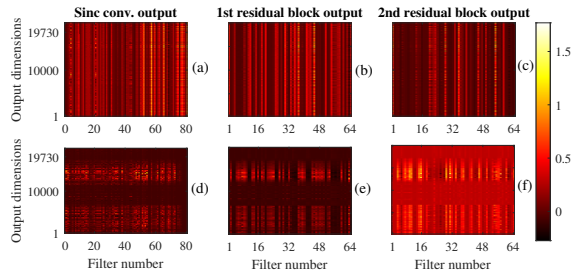


Figure 13: Visualization of the feature maps extracted from the sinc-convolution layer, first residual block, and second residual block of our proposed ILDNet for **correctly classified** healthy RS (a-c) and ILD-affected RS (d-f).

Results (contd.)

Class-specific heat-map visualization and overall performance comparison

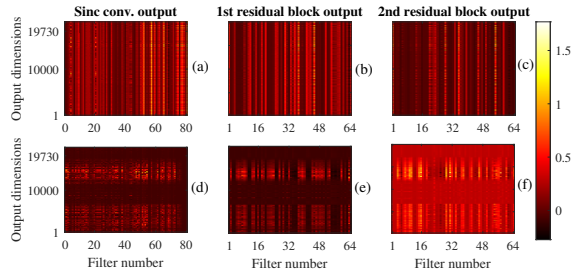


Figure 13: Visualization of the feature maps extracted from the sinc-convolution layer, first residual block, and second residual block of our proposed ILDNet for **correctly classified** healthy RS (a-c) and ILD-affected RS (d-f).

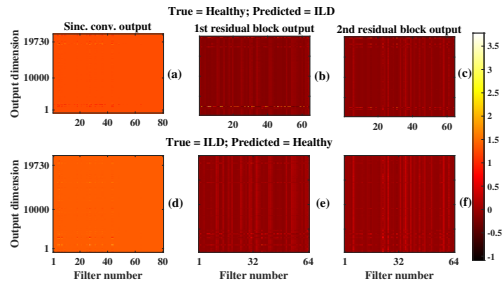


Figure 14: Visualization of the feature maps extracted from the sinc-convolution layer, first residual block, and second residual block of our proposed ILDNet for **incorrectly classified** healthy RS (a-c) and ILD-affected RS (d-f).

Results (contd.)

Class-specific heat-map visualization and overall performance comparison

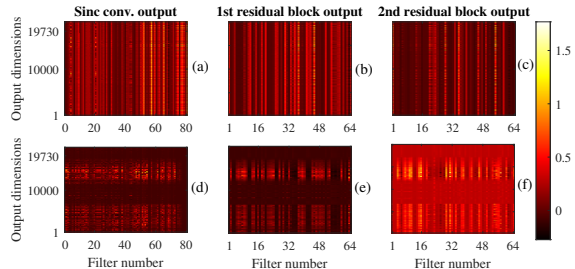


Figure 13: Visualization of the feature maps extracted from the sinc-convolution layer, first residual block, and second residual block of our proposed ILDNet for **correctly classified** healthy RS (a-c) and ILD-affected RS (d-f).

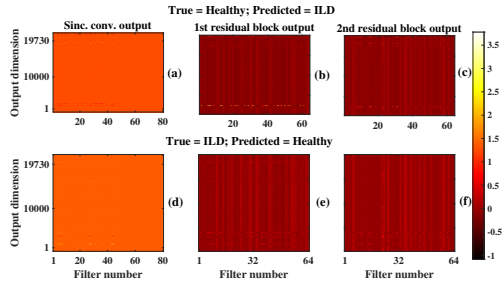


Figure 14: Visualization of the feature maps extracted from the sinc-convolution layer, first residual block, and second residual block of our proposed ILDNet for **incorrectly classified** healthy RS (a-c) and ILD-affected RS (d-f).

Table 6: Overall Comparison of Our Proposed RS-Based ILDNet Framework with Existing Works on ILD Classification using Different Diagnostic Modalities

Reference	Diagnostic modality	Methodology	Results (%)		
			ACC	SNS	SPF
Anthimopoulos et al. [1]	CT images	Five-layer CNN architecture	85.5	–	–
Martinez et al. [12]		Ensemble transfer learning based DL model	82.7	–	–
Vishraj et al. [3]	HRCT images	Haralick feature extraction, and classification using RF classifier	85.8	–	–
Proposed work	RSs [10, 9]	Framing into 5 sec window, z-score normalization, classification using ILDNet	81.25	78.85	83.33

Conclusion

- Establishes the fact that respiratory sounds play an important role in ILD detection.
- Sinc-convolution based ILDNet outperforms the baseline CNN architectures with less parameters.
- This work highlights the feasibility of developing automatic ILD detection in real-clinical scenario as an alternative diagnostic tool.

Future scope

- Quality assessment of respiratory sounds
- Denoise the signal from ambient sounds and heart sounds



References I

-  M. Anthimopoulos, S. Christodoulidis, L. Ebner, A. Christe, and S. Mougiakakou, "Lung pattern classification for interstitial lung diseases using a deep convolutional neural network," *IEEE Transactions on Medical Imaging*, vol. 35, no. 5, pp. 1207–1216, 2016.
-  Y. Ye, C.W. Sing, R. Hubbard, D. C. L. Lam, H.-L. Li, G. H.-Y. Li, S.- C. Ho, and C. L. Cheung, "Prevalence, incidence, and survival analysis of interstitial lung diseases in hong kong: a 16-year population-based cohort study," *The Lancet Regional Health–Western Pacific*, 2023.
-  R. Vishraj, S. Gupta, and S. Singh, "ECM-ILTP: An efficient classification model for categorization of interstitial lung tissue patterns," in *2021 3rd International Conference on Advances in Computing, Communication Control and Networking (ICAC3N)*, 2021, pp. 481–485.
-  J. Kebbe, T. Abdo, "Interstitial lung disease: the diagnostic role of bronchoscopy" in *J Thorac Dis.*, 2017 Sep;9(Suppl 10):S996-S1010.
-  D.C. Johnson, "Pulmonary function tests and interstitial lung disease", in *Chest*, 2021, 159(3), p.1304.
-  S. A. H. Tabatabaei, P. Fischer, H. Schneider, U. Koehler, V. Gross and K. Sohrabi, "Methods for Adventitious Respiratory Sound Analyzing Applications Based on Smartphones: A Survey," in *IEEE Reviews in Biomedical Engineering*, vol. 14, pp. 98-115, 2021.
-  A. Roy, U. Satija, "AsthmaSCELNet: A Lightweight Supervised Contrastive Embedding Learning Framework for Asthma Classification Using Lung Sounds", *Proc. INTERSPEECH 2023*, 5431-5435.
-  B. Rocha, D. Filos, L. Mendes, I. Vogiatzis, E. Perantoni, E. Kaimakamis, P. Natsiavas, A. Oliveira, C. Jacome, A. Marques et al., "A respiratory sound database for the development of automated classification," in *International Conference on Biomedical and Health Informatics*, Springer, 2017, pp. 33–37.
-  D. Pessoa, B. M. Rocha, C. Strodtthoff et al., "BRACETS: bimodal repository of auscultation coupled with electrical impedance thoracic signals," *Computer Methods and Programs in Biomedicine*, vol. 240, p. 107720, 2023.
-  M. Fraiwan, L. Fraiwan, B. Khassawneh, and A. Ibnian, "A dataset of lung sounds recorded from the chest wall using an electronic stethoscope," *Data in Brief*, vol. 35, pp. 106913, 2021.
-  M. Ravanelli and Y. Bengio, "Speaker recognition from raw waveform with SincNet," in *2018 IEEE Spoken Language Technology Workshop (SLT)*, 2018, pp. 1021–1028.
-  J. B. Martinez and G. Gill, "Comparison of pre-trained vs domain-specific convolutional neural networks for classification of interstitial lung disease," in *2019 International Conference on Computational Science and Computational Intelligence (CSCI)*, 2019, pp. 991–994.

Thank you

Any question? !?